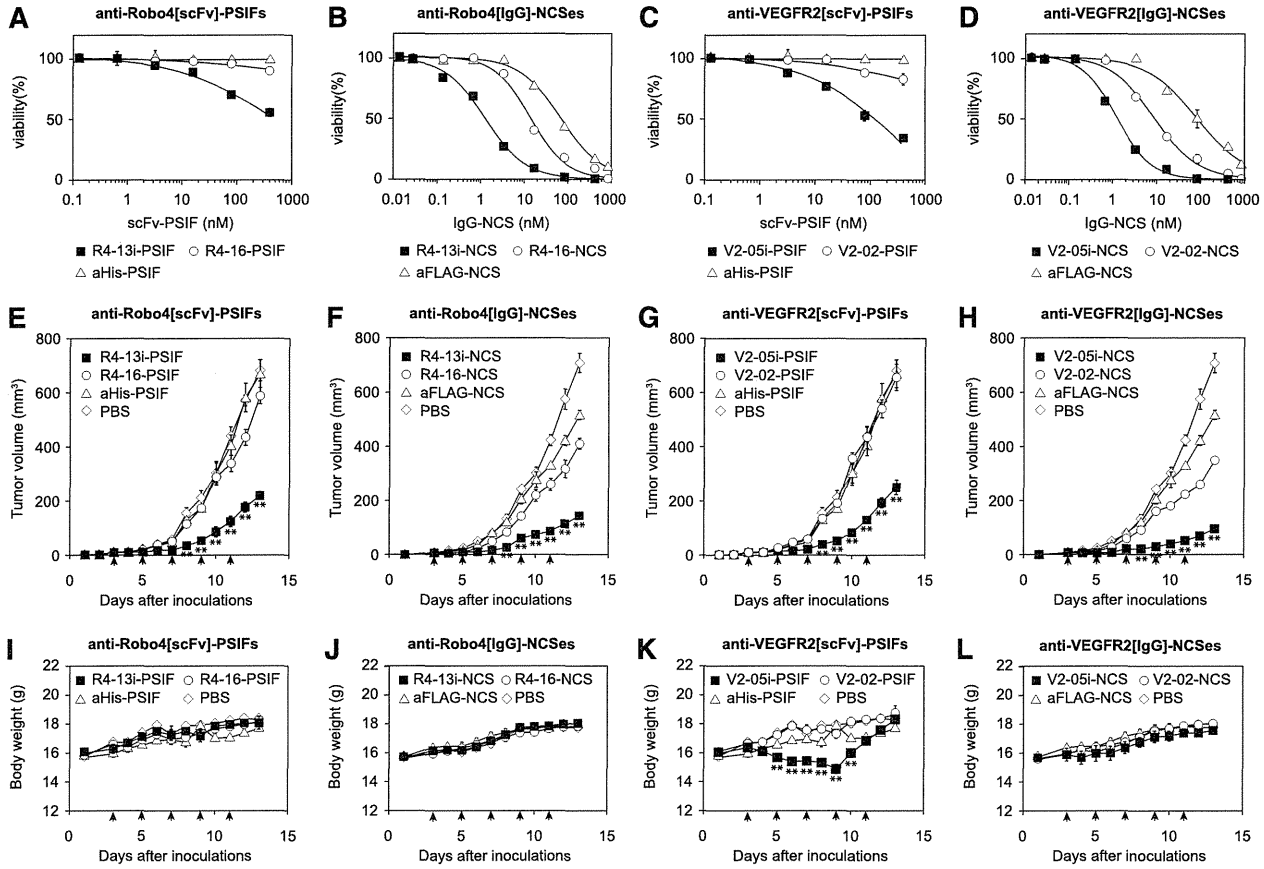

Figure 5. Enhanced anti-tumor effect of cell-internalizing mAbs. (A-D) Cytotoxicity of scFv-PSIF and IgG-NCS against MS1 cells. MS1 cells were incubated with serially diluted mAb-drug conjugates for 24 hours. Cell viability was then measured using a WST-8 assay. Closed square, internalizing mAbs; open circle, low-internalizing mAbs; open triangle, negative controls. (A) anti-Robo4[scFv]-PSIFs, (B) anti-Robo4[IgG]-NCSes, (C) anti-VEGFR2[scFv]-PSIFs, (D) anti-VEGFR2[IgG]-NCSes. Anti-His[scFv]-PSIF and anti-FLAG[IgG]-NCS were used as negative controls. Values are shown as means ± SD. (E-H) Antitumor effects of scFv-PSIFs or IgG-NCSes. B16BL6 cells were inoculated intracutaneously into C57BL6 mice on day 0. On days 3, 5, 7, 9, and 11, mAb-drug conjugates were intravenously administered *(arrow heads)*. Tumor volume was calculated using the following formula: tumor volume (mm^3) = {major axis of tumor (mm)} × {minor axis of tumor (mm)}^{2} × 0.4. Closed square, internalizing mAbs; open circle, low-internalizing mAbs; open triangle, negative controls (anti-His[scFv]-PSIF or anti-FLAG[IgG]-NCS); open diamond, PBS. (E) Anti-Robo4[scFv]-PSIFs, (F) anti-Robo4[IgG]-NCSes, (G) anti-VEGFR2[scFv]-PSIFs, (H) anti-VEGFR2[IgG]-NCSes. Values are shown as means ± SEM. $^{**}P < 0.01$; internalizing mAbs versus low-internalizing mAbs by Bonferroni post hoc analysis with two-way ANOVA (n = 6). (I-L) Change in body weight during therapy experiment. Closed square, internalizing mAbs; open circle, low-internalizing mAbs; open triangle, negative controls (anti-His[scFv]-PSIF or anti-FLAG[IgG]-NCS); open diamond, PBS. (I) anti-Robo4[scFv]-PSIFs, (J) anti-Robo4[IgG]-NCSes, (K) anti-VEGFR2[scFv]-PSIFs, (L) anti-VEGFR2[IgG]-NCSes. Values are shown as means ± SEM. $^{**}P < 0.01$; internalizing mAbs versus PBS by Bonferroni post hoc analysis with two-way ANOVA (n = 6).

human phage antibody libraries,[46,47] which have already been developed. This system can expand the versatility of phage display systems, which will thus contribute to the development of other cell-internalizing antibodies against various types of antigens for effective cancer therapy.

A comparison of cell-internalizing mAbs with low-internalizing mAbs revealed the strength of the cell-internalizing mAbs in terms of the biodistribution and therapeutic effects. Until now, how internalization contributes to the biodistribution of mAbs has been unclear. In this report, we could use a comparative study to clarify this question because we produced both cell-internalizing mAbs and low-internalizing mAbs with similar binding affinities. As a result, more cell-internalizing mAbs than low-internalizing mAbs were significantly accumulated in the tumor. This is the first evidence to support that mAbs with high internalization activity have greater tumor-targeting potency. This information is also useful for other applications that benefit from cell-internalizing mAbs, such as liposomal drugs, bioactive proteins/peptides, and viral vectors.[48,49]

Until now, the usefulness of Robo4-targeted therapy has not been established. Therapy to target VEGF-VEGFR signaling is already common, but the risk of side effects must be addressed.[31-33] Although VEGFR expression is upregulated on tumor vessels, it is also observed on the endothelium in healthy tissues. Previous reports also mentioned the toxicity associated with the anti-VEGFR therapies in mouse models[50] and the clinical trial.[51] Therefore, alternative therapies that target tumor angiogenesis are desired. In the present study, we revealed the possibility that anti-Robo4 ADCs were safer than anti-VEGFR2 ADCs, although they had similar antitumor effects. The findings from immunofluorescence and biodistribution studies also support the notion that anti-Robo4 mAbs could accumulate in the tumor without distributing to normal tissues. This is the first finding of Robo4-targeted therapy and suggests that Robo4 is a potential alternative target for tumor vascular targeting. Of course, additional experiments are needed to establish anti-Robo4 as a novel tool in tumor vascular targeting. For example, the pathological observations of normal blood vessels, in-depth toxicological analysis,

or the efficacy against other clinical relevant tumor models, are important for the successful story. Such basic analyses regarding Robo4 might accelerate the development of novel medicines that target tumor angiogenesis, including anti-Robo4 ADCs.

Acknowledgments

This study was supported by Grant-in-Aid for Scientific research (B) and Grant-in-Aid for Scientific Research on Innovative Areas from the Ministry of Education, Culture, Sports, Science, and Technology of Japan and the Japan Society for the Promotion of Science; Strategic Japanese-Swiss Cooperative Program from Japan Science and Technology Agency (JST) and the Swiss Federal Institute of Technology Zurich.

Authorship

Contribution: Y.M. designed the study; M.Y. and Y. Tsumori performed the experiments; Y.M. and M.Y. analyzed the data; Y.M. and M.Y. wrote the initial manuscript; S.T. and Y. Tsutsumi contributed to the phage display; Y.Y. and N.O. contributed to animal experiments; Y.O., W.C.A., and T.D. contributed to Robo4 related analysis; Y.M. and S.N. were responsible for the overall project. All authors edited the manuscript.

Conflict-of-interest disclosure: The authors declare no competing financial interests.

Correspondence: Yohei Mukai and Shinsaku Nakagawa, Laboratory of Biotechnology and Therapeutics, Graduate School of Pharmaceutical Sciences, Osaka University, 1–6 Yamadaoka, Suita, Osaka 565–0871, Japan; e-mail: y-mukai@nibio.go.jp and nakagawa@phs.osaka-u.ac.jp.

References

1. Alley SC, Okeley NM, Senter PD. Antibody-drug conjugates: targeted drug delivery for cancer. *Curr Opin Chem Biol.* 2010;14(4):529-537.
2. Isakoff SJ, Baselga J. Trastuzumab-DM1: building a chemotherapy-free road in the treatment of human epidermal growth factor receptor 2-positive breast cancer. *J Clin Oncol.* 2011;29(4): 351-354.
3. Ansell SM. Brentuximab vedotin: delivering an antimitotic drug to activated lymphoma cells. *Expert Opin Investig Drugs.* 2011;20(1):99-105.
4. Reichert JM. Antibody-based therapeutics to watch in 2011. *MAbs.* 2011;3(1):76-99.
5. Gerber HP, Senter PD, Grewal IS. Antibody drug-conjugates targeting the tumor vasculature: Current and future developments. *MAbs.* 2009; 1(3):247-253.
6. Poul MA, Becerril B, Nielsen UB, et al. Selection of tumor-specific internalizing human antibodies from phage libraries. *J Mol Biol.* 2000;301(5): 1149-1161.
7. An F, Drummond DC, Wilson S, et al. Targeted drug delivery to mesothelioma cells using functionally selected internalizing human single-chain antibodies. *Mol Cancer Ther.* 2008;7(3): 569-578.
8. Mukai Y, Sugita T, Yamato T, et al. Creation of novel Protein Transduction Domain (PTD) mutants by a phage display-based high-throughput screening system. *Biol Pharm Bull.* 2006;29(8):1570-1574.
9. Chaudhary VK, FitzGerald DJ, Adhya S, et al. Activity of a recombinant fusion protein between transforming growth factor type alpha and Pseudomonas toxin. *Proc Natl Acad Sci USA.* 1987;84(13):4538-4542.
10. Kreitman RJ, Wilson WH, Bergeron K, et al. Efficacy of the anti-CD22 recombinant immunotoxin BL22 in chemotherapy-resistant hairy-cell leukemia. *N Engl J Med.* 2001;345(4): 241-247.
11. Pastan I, FitzGerald D. Pseudomonas exotoxin: chimeric toxins. *J Biol Chem.* 1989;264(26): 15157-15160.
12. Legg JA, Herbert JMJ, Clissold P, et al. Slits and Roundabouts in cancer, tumour angiogenesis and endothelial cell migration. *Angiogenesis.* 2008; 11(1):13-21.
13. Huminiecki L, Bicknell R. In silico cloning of novel endothelial-specific genes. *Genome Res.* 2000; 10(11):1796-1806.
14. Huminiecki L, Gorn M, Suchting S, et al. Magic roundabout is a new member of the roundabout receptor family that is endothelial specific and expressed at sites of active angiogenesis. *Genomics.* 2002;79(4):547-552.
15. Smith-Berdan S, Nguyen A, Hassanein D, et al. Robo4 cooperates with CXCR4 to specify hematopoietic stem cell localization to bone marrow niches. *Cell Stem Cell.* 2011;8(1):72-83.
16. Park KW, Morrison CM, Sorensen LK, et al. Robo4 is a vascular-specific receptor that inhibits endothelial migration. *Dev Biol.* 2003;261(1): 251-267.
17. Seth P, Lin Y, Hanai J, et al. Magic roundabout, a tumor endothelial marker: expression and signaling. *Biochem Biophys Res Commun.* 2005; 332(2):533-541.
18. Okada Y, Yano K, Jin E, et al. A three-kilobase fragment of the human Robo4 promoter directs cell type-specific expression in endothelium. *Circ Res.* 2007;100(12):1712-1722.
19. Okada Y, Jin E, Nikolova-Krstevski V, et al. A GABP-binding element in the Robo4 promoter is necessary for endothelial expression in vivo. *Blood.* 2008;112(6):2336-2339.
20. Jones CA, London NR, Chen H, et al. Robo4 stabilizes the vascular network by inhibiting pathologic angiogenesis and endothelial hyperpermeability. *Nat Med.* 2008;14(4):448-453.
21. Jones CA, Nishiya N, London NR, et al. Slit2-Robo4 signalling promotes vascular stability by blocking Arf6 activity. *Nat Cell Biol.* 2009; 11(11):1325-1331.
22. Marlow R, Binnewies M, Sorensen LK, et al. Vascular Robo4 restricts proangiogenic VEGF signaling in breast. *Proc Natl Acad Sci USA.* 2010;107(23):10520-10525.
23. Koch AW, Mathivet T, Larrivée B, et al. Robo4 maintains vessel integrity and inhibits angiogenesis by interacting with UNC5B. *Dev Cell.* 2011;20(1):33-46.
24. Kerbel RS. Tumor angiogenesis. *N Engl J Med.* 2008;358(19):2039-2049.
25. Paleolog EM. Angiogenesis in rheumatoid arthritis. *Arthritis Res.* 2002;4(Suppl 3):S81-S90.
26. Tonnesen MG, Feng X, Clark RA. Angiogenesis in wound healing. *J Investig Dermatol Symp Proc.* 2000;5(1):40-46.
27. Olsson AK, Dimberg A, Kreuger J, et al. VEGF receptor signalling - in control of vascular function. *Nat Rev Mol Cell Biol.* 2006;7(5):359-371.
28. Crawford Y, Ferrara N. VEGF inhibition: insights from preclinical and clinical studies. *Cell Tissue Res.* 2009;335(1):261-269.
29. Wicki A, Rochlitz C, Orleth A, et al. Targeting tumor-associated endothelial cells: anti-VEGFR2 immunoliposomes mediate tumor vessel disruption and inhibit tumor growth. *Clin Cancer Res.* 2012;18(2):454-464.
30. Witmer AN, Dai J, Weich HA, et al. Expression of vascular endothelial growth factor receptors 1, 2, and 3 in quiescent endothelia. *J Histochem Cytochem.* 2002;50(6):767-777.
31. Kamba T, McDonald DM. Mechanisms of adverse effects of anti-VEGF therapy for cancer. *Br J Cancer.* 2007;96(12):1788-1795.
32. Eremina V, Jefferson JA, Kowalewska J, et al. VEGF inhibition and renal thrombotic microangiopathy. *N Engl J Med.* 2008;358(11):1129-1136.
33. Choueiri TK, Mayer EL, Je Y, et al. Congestive heart failure risk in patients with breast cancer treated with bevacizumab. *J Clin Oncol.* 2011; 29(6):632-638.
34. Yoshikawa M, Mukai Y, Okada Y, et al. Ligand-independent assembly of purified soluble magic roundabout (Robo4), a tumor-specific endothelial marker. *Protein Expr Purif.* 2008;61(1):78-82.
35. Imai S, Mukai Y, Nagano K, et al. Quality enhancement of the non-immune phage scFv library to isolate effective antibodies. *Biol Pharm Bull.* 2006;29(7):1325-1330.
36. Yoshikawa M, Mukai Y, Tsunoda S, et al. Modifying the antigen-immunization schedule improves the variety of monoclonal antibodies obtained from immune-phage antibody libraries against HIV-1 Nef and Vif. *J Biosci Bioeng.* 2011; 111(5):597-599.
37. Yamamoto Y, Tsutsumi Y, Yoshioka Y, et al. Site-specific PEGylation of a lysine-deficient TNF-alpha with full bioactivity. *Nat Biotechnol.* 2003;21(5):546-552.
38. Hunter WM, Greenwood FC. Preparation of iodine-131 labelled human growth hormone of high specific activity. *Nature.* 1962;194:495-496.
39. Mellman I. Endocytosis and molecular sorting. *Annu Rev Cell Dev Biol.* 1996;12:575-625.
40. Holliger P, Hudson PJ. Engineered antibody fragments and the rise of single domains. *Nat Biotechnol.* 2005;23(9):1126-1136.
41. Pavlinkova G, Beresford GW, Booth BJ, et al. Pharmacokinetics and biodistribution of engineered single-chain antibody constructs of MAb CC49 in colon carcinoma xenografts. *J Nucl Med.* 1999;40(9):1536-1546.
42. Schneider DW, Heitner T, Alicke B, et al. In vivo biodistribution, PET imaging, and tumor accumulation of 86Y- and 111In-antimindin/RG-1,

engineered antibody fragments in LNCaP tumor-bearing nude mice. *J Nucl Med.* 2009; 50(3):435-443.

43. Maeda H. SMANCS and polymer-conjugated macromolecular drugs: advantages in cancer chemotherapy. *Adv Drug Deliv Rev.* 2001;46(1-3): 169-185.

44. Kappen LS, Goldberg IH. Activation and inactivation of neocarzinostatin-induced cleavage of DNA. *Nucleic Acids Res.* 1978; 5(8):2959-2967.

45. Okamoto T, Mukai Y, Yoshioka Y, et al. Optimal construction of non-immune scFv phage display libraries from mouse bone marrow and spleen established to select specific scFvs efficiently binding to antigen. *Biochem Biophys Res Commun.* 2004;323(2): 583-591.

46. Silacci M, Brack S, Schirru G, et al. Design, construction, and characterization of a large synthetic human antibody phage display library. *Proteomics.* 2005;5(9): 2340-2350.

47. Villa A, Lovato V, Bujak E, et al. A novel synthetic naïve human antibody library allows the isolation of antibodies against a new epitope of oncofetal fibronectin. *MAbs.* 2011; 3(3):264-272.

48. Sapra P, Allen TM. Internalizing antibodies are necessary for improved therapeutic efficacy of antibody-targeted liposomal drugs. *Cancer Res.* 2002;62(24):7190-7194.

49. Pastan I, Hassan R, Fitzgerald DJ, et al. Immunotoxin therapy of cancer. *Nat Rev Cancer.* 2006;6(7):559-565.

50. Chinnasamy D, Yu Z, Theoret MR, et al. Gene therapy using genetically modified lymphocytes targeting VEGFR-2 inhibits the growth of vascularized syngenic tumors in mice. *J Clin Invest.* 2010;120(11):3953-3968.

51. Nagayama H, Matsumoto K, Isoo N, et al. Gastrointestinal bleeding during anti-angiogenic peptide vaccination in combination with gemcitabine for advanced pancreatic cancer. *Clin J Gastroenterol.* 2010;3(6):307-317.

Laboratory of Biopharmaceutical Research[1], National Institute of Biomedical Innovation; Laboratory of Toxicology and Safety Science[2], Graduate School of Pharmaceutical Sciences, Osaka University; The Center for Advanced Medical Engineering and Informatics[3], Osaka University; Department of Biochemistry[4], Osaka Medical Center for Cancer and Cardiovascular Diseases; Section of Laboratory Equipment[5], National Institute of Biomedical Innovation; Laboratory of Biomedical Innovation[6], Graduate School of Pharmaceutical Sciences, Osaka University, Osaka, Japan

Epidermal growth factor receptor localized to exosome membranes as a possible biomarker for lung cancer diagnosis

T. YAMASHITA[1,2,*], H. KAMADA[1,3,*], S. KANASAKI[1,2], Y. MAEDA[1,2], K. NAGANO[1], Y. ABE[1], M. INOUE[1], Y. YOSHIOKA[1,2,3], Y. TSUTSUMI[1,2,3], S. KATAYAMA[1,5], M. INOUE[4], S. TSUNODA[1,3,5,6]

Received March 11, 2013, accepted April 26, 2013

Shin-ichi Tsunoda, Ph.D, Laboratory of Biopharmaceutical Research, National Institute of Biomedical Innovation, 7-6-8 Saito-Asagi, Ibaraki, Osaka 567-0085, Japan.
tsunoda@nibio.go.jp
[*] *These authors contributed equally to the work.*

Pharmazie 68: 969–973 (2013) *doi: 10.1691/ph.2013.3599*

Detection of drug-target proteins and biomarkers that are expressed in cancer tissue has significant potential for both diagnosis and treatment of cancer. However, current immuno-histochemical and cytogenetic analyses of biopsy specimens for pre-operational diagnosis are highly invasive and often difficult to apply to lung cancer patients. The purpose of this study was to evaluate the possible utility of determining epidermal growth factor receptor (EGFR) expression on exosomal membranes using a targeted ELISA with an anti-CD81 antibody as a capture antibody for lung cancer diagnosis. While soluble EGFR (sEGFR) levels in plasma were not remarkably different between lung cancer patients and normal controls, significantly higher exosomal EGFR expression levels were observed in 5/9 cancer cases compared to normal controls. These results suggest that measurement of exosomal protein levels could be useful for *in vitro* diagnosis, and that exosomal EGFR is a possible biomarker for characterization of lung cancer.

1. Introduction

Lung cancer has been recognized as a heterogeneous disease, since its development is unique in terms of clinical characterizations, prognosis, response and tolerance to treatment for every patient. Epidermal growth factor receptor (EGFR) expression is significantly elevated in some of the tumors and has been associated with tumor growth, invasion, and metastasis in non-small cell lung cancer. The function of EGFR is up-regulated in lung cancers and thus its blockade by EGFR tyrosine kinase inhibitors (TKI) improves outcomes for lung cancer patients. Therefore expression of EGFR could possibly serve as a marker to predict which lung cancer patients would be most likely benefit from such a treatment (Philip et al. 2011; Gusterson et al. 1984; Modjtahedi et al. 1993). Although tumor biopsy is currently recommended as the standard method to detect EGFR expression in patients, it has several disadvantages such as its high invasiveness, potential sampling error and risk of trauma. Considering these limitations, there is a need to develop novel and less invasive methods to detect lung cancer.

Exosomes are endogenous nano-vesicles (40–100 nm in diameter) secreted by various cells (Deng et al. 2012; Simons and Raposo 2009; Théry et al. 2009) and they are known to contain many kinds of RNAs and proteins derived from their parent cells. Micro RNAs (miRNAs) included in blood exosomes could potentially be used for cancer diagnosis (Kosaka et al. 2010). The membranes of exosomes secreted from cancer cells contain proteins related to characteristics of specific cancers such as melanoma and colon cancer (Mathivanan et al. 2010; Simpson et al. 2008). These observations support the idea that detection of exosomal EGFR as a blood biomarker could prove useful for cancer diagnosis and characterization. In this study, we established a simple ELISA method to detect and quantify exosomal EGFR. We also examined the possibility of utilizing exosomal EGFR as a blood biomarker for lung cancer diagnosis. Our demonstration of exosomal EGFR in the plasma from a lung cancer patient provides a rationale for further studies to investigate the utility of exosomal EGFR as an easily measurable biomarker for lung cancer diagnosis.

2. Investigations and results

2.1. Characteristics of exosomes derived from HPAEpiC and HARA-B cell lines

Exosomes derived from HPAEpiC and HARA-B cells were compared using transmission electron microscopy (TEM) and dynamic light scattering. Electron microscopy analysis revealed that the exosomes collected from the culture medium of various cancer cell lines consisted primarily of small membrane vesicles having an average diameter of 90–120 nm (Fig. 1A, 1B), similar to previously described exosome preparations (Valadi et al. 2007).

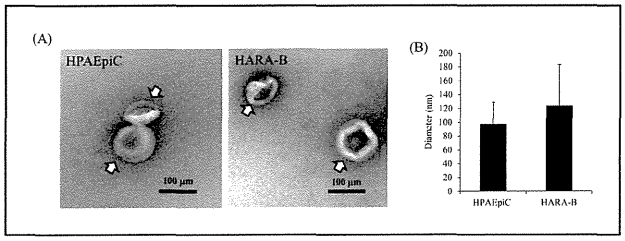

Fig. 1: Characteristics of purified exosomes. A) TEM images of exosomes derived from HPAEpiC and HARA-B cells negatively stained with uranyl acetate. B) The average diameters of exosomes. The average particle diameters obtained by dynamic light scattering. Data are shown as means and standard deviations of 6 measurements.

2.2. Comparison of EGFR expression between cancer cell lines

In order to select lung cancer cells that expressed EGFR at high levels, western blots were performed for cancer cell lines and HPAEpiC cells (Fig. 2A). Quantitative analysis revealed that lung cancer cell lines expressed EGFR while EGFR was seldom detected on HPAEpiC cells. EGFR expression was particularly high on HARA-B cells (Fig. 2B). Furthermore, EGFR expression levels were parallel on exosomes and the cells from which they were derived (Fig. 2B and 2C).

2.3. Expression analysis of exosomal EGFR derived from conditioned media and plasma of tumor-bearing mice

Detection, quantification and characterization of target molecules by a blood test is ideal for performing a cancer diagnosis. To determine whether EGFR was expressed on the exosomes derived from cancer cells and whether this could be a useful biomarker indicating the presence or the expression level of the cancer-related molecules of cancer, exosomal EGFR levels in conditioned media and plasma from tumor-bearing mice were measured by an ELISA assay. At first, purified exosomes derived from cell culture supernatants were captured using an anti-human CD81 antibody. Furthermore, Figs. 3A and 3B show that EGFR in cell supernatants and purified exosomes derived from HARA-B cells, which showed the highest levels of EGFR among the examined cell lines (Fig. 2C), were detected in a dose-dependent manner. In contrast, EGFR expression on exosomes derived from HPAEpiC cells was almost undetectable. Thus, exosomal EGFR expression in cell supernatants could be assessed by this ELISA system. Next, the exosomal EGFR levels in plasma of HARA-B tumor-bearing mice were investigated. Expression of EGFR in HARA-B tumor tissue was confirmed by immunostaining using an anti-human EGFR antibody (Fig. 3C). The plasma samples of the tumor-bearing mice were measured using an established ELISA, and then exosomal EGFR levels were found to increase in parallel with the tumor size (Fig. 3D). These results indicate that detection of exosomal EGFR levels in plasma could be used to estimate the sizes of tumors.

2.4. Comparison of soluble and exosomal EGFR levels in human plasma

A previous study has indicated that sEGFR is not a useful blood biomarker for lung cancer diagnosis because it is detected in blood from both healthy individuals and cancer patients (Jacot et al. 2004). Therefore, in order to evaluate the possible utility of exosomal EGFR as a lung cancer biomarker, we compared the expression levels of soluble and exosomal EGFR in plasma from nine lung cancer patients and from normal controls. The sEGFR levels did not differ remarkably between normal and lung cancer

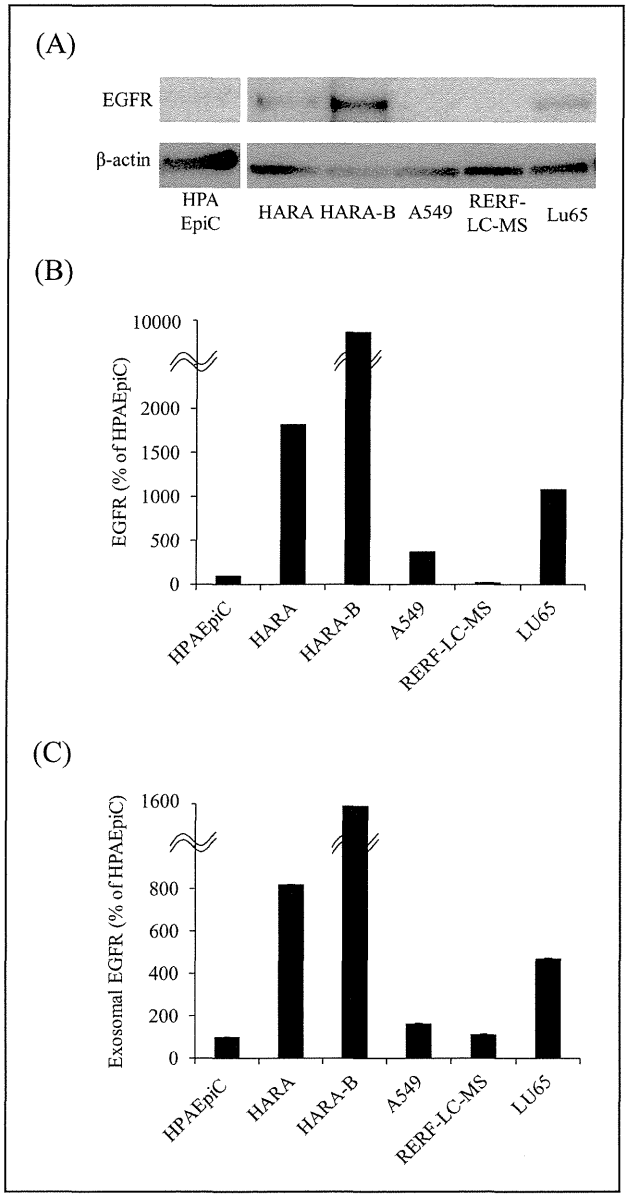

Fig. 2: Expression of EGFR on cancer cell-derived exosomes. A) Western blotting analysis of EGFR expression in lysates from lung cancer cell lines. B) Quantitative analysis of the Western blotting results of A. Signal quantification was performed by densitometry with normalization by b-actin. C) Expression of EGFR on exosomes in conditioned media. Ultracentrifuge-purified exosomes derived from the indicated cells were captured by anti-CD81 and detected by anti-EGFR. Data are shown as means and standard deviations (n = 3).

patient plasma. On the other hand, exosomal EGFR was significantly higher in five lung cancer patients plasma compared to healthy controls.

3. Discussion

Several blood biomarkers are commonly used for clinical cancer detection, e.g., carcinoembryonic antigen (CEA) and cytokeratin 19 fragment (CYFRA 21–1) for lung cancer (MacSween et al. 1972; Pujol et al. 1993). However, these biomarkers show low specificity and poor capability to detect tumors, although they continue to be used for cancer diagnosis. There is a clear need for improved biomarkers with higher specificity for cancer diagnosis and therapy. EGFR is known to be a good biomarker for lung cancer because it is highly expressed in tumor tissue

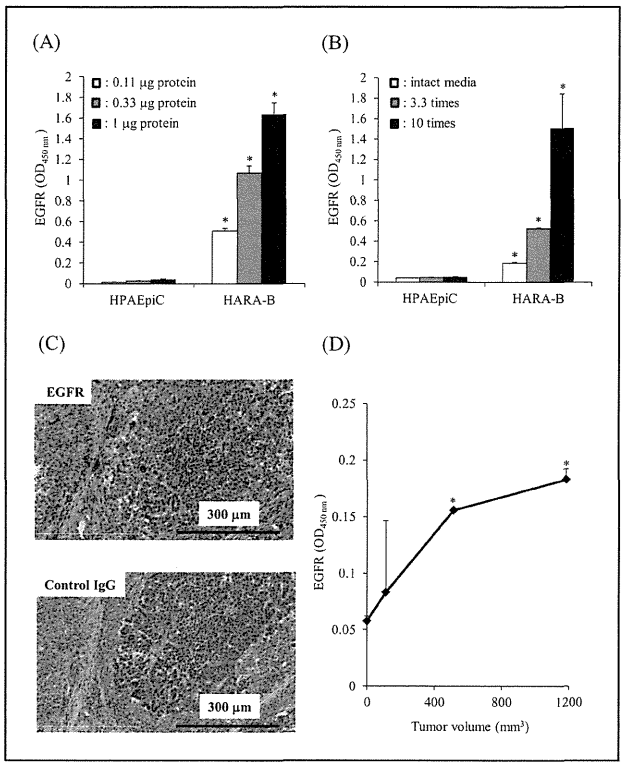

Fig. 3: Exosomal EGFR derived from conditioned medium and plasma from tumor-bearing mice. A) Concentration dependence analysis of EGFR expression on ultracentrifuge-purified exosomes (0.11, 0.33 and 1.0 μg exosomal protein) derived from HARA-B cells. Exosomes were captured and detected using an anti-CD81 antibody B) EGFR expression in exosomes derived from conditioned media of HARA-B cells (intact and concentrated 3 and 10 times by ultrafiltration). Exosomes were captured by an anti-CD81 antibody and then detected using an anti-EGFR antibody. C) Expression of EGFR on HARA-B xenograft tumors. The HARA-B tumor sections were stained using an anti-EGFR antibody. Isotype control staining was also performed. Representative 200x photomicrographs are shown. D) Relationship between plasma levels of CD81 + /EGFR + exosomes and tumor volume. Plasma samples were collected from mice sacrificed 10, 17 and 21 days after inoculation with HARA-B cells. Data are shown as means and standard deviations (n = 3).

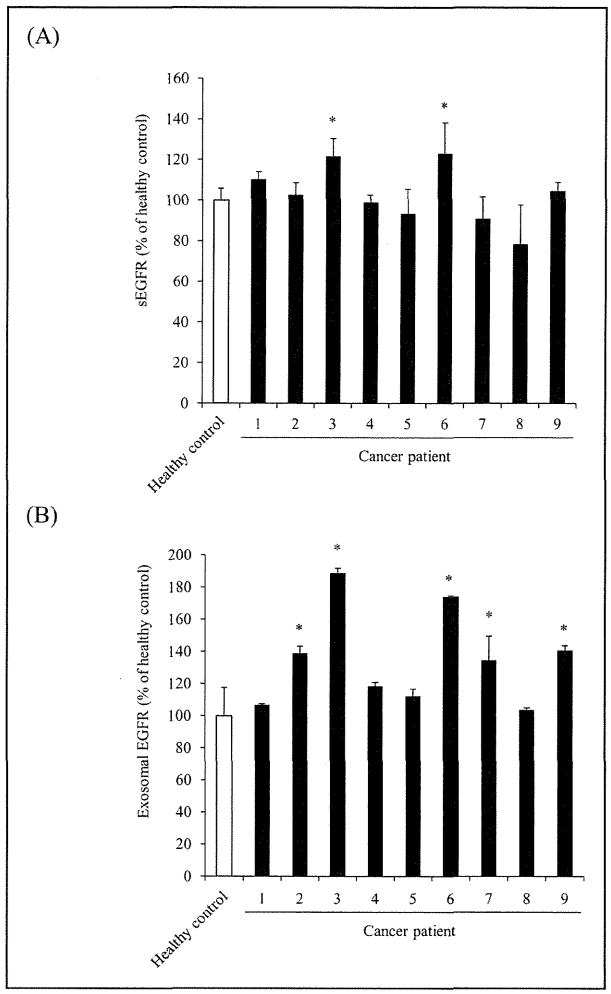

Fig. 4: Expression of sEGFR and exosomal EGFR in human plasma from lung cancer patients. A) Expression analysis of sEGFR using an ELISA, which consisted of two different antibodies recognizing other epitopes of EGFR. B) Expression analysis of exosomal EGFR using an ELISA, which utilized anti-EGFR and anti-CD81 antibodies. Exosomes were captured by an anti-CD81 antibody and then detected using an anti-EGFR antibody. Data are shown as means and standard deviations (n = 3). *$P < 0.05$ (vs. normal).

and also is a target molecule of EGFR TKIs, which are used to treat lung cancer patients. However, EGFR expression is evaluated by performing a biopsy that is highly invasive, and it would be quite desirable to develop a less invasive method to quantify it. The present study demonstrates that exosomal EGFR is a possible biomarker for lung cancer detection and characterization, and its expression may be evaluated by an EGFR-targeted ELISA using an anti-CD81 antibody as a capture antibody. This ELISA system should be capable of detecting EGFR on membranes of exosomes. This diagnostic method could be applied to lung cancer detection and pharmacometrics analysis, etc.

A previous report showed that the levels of exosomes in blood derived from cancer patients are higher than in healthy persons (Taylor and Gercel-Taylor 2008). Therefore, an ELISA system could be used for lung cancer diagnostics if EGFR was expressed at higher levels on exosomes from lung cancer patients. However, it has been reported that sEGFR levels are similar in blood from lung cancer patients and normal controls. Furthermore, exosomes are detected in plasma from healthy individuals as well as from cancer patients because they are secreted from various cells in normal and disease situations (Fevrier et al. 2004; Witek et al. 2009). Therefore, the tumor-derived exosomes must be distinguished from other exosomes for diagnostic purposes. The results of our animal study indicate that exosomes in plasma that express high levels of EGFR are clearly derived from tumor tissue, because this mouse model was inoculated with a human lung cancer cell line and the ELISA system can only detect human CD81 and human EGFR. Furthermore, our results indicate that exosomal EGFR detection could potentially be used in blood tests to diagnose lung cancer because the exosomal EGFR level was higher in lung cancer patients than in normal individuals (Fig. 4).

It is thought that secretion of exosomal EGFR derived from tumor tissue is increased in lung cancer patients. However, the present study did not reveal any relationship between EGFR expression levels in exosomes *versus* tumor tissues. Further studies are necessary to investigate the relationships among size, stage, EGFR expression of tumor tissues and plasma exosomal EGFR levels. Future large-scale validation studies are also anticipated. Tetraspanins such as CD9, CD63 and CD81 are a family of small proteins expressed on membranes. They are highly enriched in late endosomes, lysosomes, and multi-vesicular bodies, where they associate to form complexes (Andre et al. 2002; Abache et al. 2007; Pols and Klumperman 2009). Secretion of exosomes from dendritic cells of CD9 knockout mice was found to be reduced (Chairoungdua et al. 2010), suggesting that tetraspanins are essential molecules for generation of exosomes. Another study utilized an anti-CD63 antibody and caveolin-1 antibodies to detect endosomes in plasma from melanoma

patients (Logozzi et al. 2009). CD63-positive exosomes were found to be highly expressed in *in vitro* culture supernatants and were also detected in plasma from melanoma patients. In contrast, we carried out a proteomics study to determine what kinds of tetraspanins were expressed on exosomes derived from lung cancer cell lines. The results indicated that exosomal CD63 was seldom detected in some lung cancer cells but CD81 was widely expressed (in the lines HARA, HARA-B, A549, and LU65). Chiba et al. also reported that CD81 was widely expressed on exosomes derived from colon cancer cell lines (HCT-15, SW480, and WiDr), as indicated by western blotting experiments (Chiba et al. 2012). Furthermore, it was reported that CD81 promotes cell proliferation by ERK/MAP Kinase activation and tyrosine phosphorylation in hepatocellular carcinoma cells (Carloni et al. 2004). Thus, CD81 may be useful as an appropriate marker for exosomes derived from cancer cells.

This study demonstrates for the first time that exosomal EGFR may be detected and quantified using CD81 and EGFR targeted ELISA assays. The alteration of plasma EGFR concentration in cancer patients could be detected by a targeted ELISA capturing exosomes because soluble EGFR is usually observed in the healthy state. Although this ELISA system could be useful for cancer detection, optimization of this method (e.g. exploitation of radio-isotopes or fluorescence, affinity maturation of antibodies, etc.) will be needed to estimate EGFR expression levels in cancer tissues.

It has been reported that tumor-specific gene mutations of EGFR could be detected by reverse transcription-PCR analysis in serum vesicles from glioblastoma patients (Skog et al. 2008). The exosomes include not only tumor derived membrane or cytosolic proteins but also mRNA expressed in tumor cells. In the future, exosome analysis, which allows simultaneous measurement of EGFR gene mutations and EGFR protein expression, will likely provide more valuable information for diagnosis and to inform therapeutic decisions for cancer patients, compared to previous methods.

4. Experimental

4.1. Cell lines

HARA, HARA-B, A549, RERF-LC-MS and LU65 cells were purchased from the JCRB cell bank. HARA, HARA-B and LU65 cells were maintained in RPMI1640 medium containing 10% fetal calf serum (FCS). A549 and RERF-LC-MS cells were maintained in Eagle's minimal essential medium with non-essential amino acids containing 10% FCS under a 5% CO_2 atmosphere at 37 °C. Primary human pulmonary alveolar epithelial cells (HPAEpiC) were purchased from Science Cell Research Laboratory. These cells were maintained in Alveolar Epithelial Cell Medium (Science Cell Research Laboratory, California, USA) under a 5% CO_2 atmosphere at 37 °C.

4.2. Electron microscopy

Electron microscope images of exosomes were taken by floating a carbon-coated 400-mesh Formvar EM grid on top of 5 µl of freshly prepared exosomes in deionized water for 20 min. The grid was then briefly washed with deionized water and floated on a drop of 2% uranyl acetate. Samples were examined using an H-7650 Transmission Electron Microscope (Hitachi High-Technologies).

4.3. Preparation of conditioned media and exosomes

Prior to exosomes collection, confluent cells were incubated for 72 h without FCS. Exosomes were prepared from the supernatant of lung cancer cells and HPAEpiC by centrifugation. Six hundred ml volumes of supernatants containing 1 x 10^8 HPAEpiC or 6 x 10^8 lung cancer cells were centrifuged at 300 g for 5 min to eliminate cells and at 16,000 x g for 20 min, followed by filtration through a 0.22 µm filter to clear cell debris. Exosomes were precipitated by ultracentrifugation at 140,000 x g for 70 min. The pellets of exosomes were washed once in PBS and their protein contents were measured using a Micro BCA protein assay kit (Thermo Fisher Scientific). Particle sizes were measured by dynamic light scattering using a Zetasizer nano (Malvern).

4.4. Western blots

All cells were lysed in RIPA buffer (Thermo Fisher Scientific) containing Complete Protease Inhibitor Cocktail (Roche Diagnostics). Determination of protein concentrations was performed using a micro BCA protein assay kit (Thermo Fisher Scientific). Cell lysates were electrophoresed in 10% SDS-polyacrylamide gels (10 µg/ lanes) and transferred to PVDF membranes (Millipore). After blocking with 4% Block Ace (DS Pharma Biomedical) for 60 min at room temperature, the blots were reacted with anti-EGFR polyclonal antibody (clone AF231, R&D Systems) in a buffer containing 0.4% block ace, and then with an HRP conjugated anti-goat IgG secondary antibody (Jackson Immuno Research) in the same buffer and detected using the ECL-plus system (GE Healthcare). Equal amounts of protein loading were confirmed by parallel β-actin immunoblotting, and signal quantification was performed by densitometric scanning.

4.5. Detection of exosomes in plasma and conditioned media using targeted ELISA with anti CD81 and anti EGFR antibody

Ninety-six well Maxisorp plates (Nunc) were coated with 20 µg/ml mouse anti human CD81 monoclonal antibody (clone 1D6, Gene Tex) in volumes of 100 µl/well of carbonate buffer (pH 9.6) and incubated overnight at 4 °C. After incubation, 100 µl/well of 4% BLOCK ACE (DS-pharma) were added and incubated overnight at 4 °C. After 3 washes with PBS, several concentrations of purified exosomes, conditioned media and mouse or human plasma were added to a final volume of 100 µl and incubated for 60 min at 37 °C. Sample concentrations are given in the figure legends. After 3 washes with PBS, 0.8 µg/ml goat anti-human EGFR polyclonal antibody was added and incubated for 60 min at 37 °C. After 3 washes with PBS, the plates were incubated with 100 µl of HRP-conjugated anti-goat IgG antibody per well diluted 1:5,000 in 0.4% block ace for 60 min at room temperature. After the final 3 washes with PBS, the reaction was developed with tetramethyl benzidine reagents, blocked with H_2SO_4 and optical densities were recorded at 450 nm. Human plasma samples were purchased from Kohjin Bio (Saitama, Japan: healthy control) and Tissue Solutions Ltd (Glasgow, UK: lung cancer samples). Soluble EGFR (sEGFR) was detected by EGFR Human ELISA kit (R & D Systems).

4.6. Human tumor xenograft mice model

Six-week-old male BALB/c Slc-nu/nu mice (Japan SLC) were maintained at the animal care facility of National Institute of Biomedical Innovation under a regulated protocol. A suspension of HARA-B cells (1 x 10^6 cells/mouse) was inoculated s.c. into the backs of the mice. The two perpendicular diameters of the tumors were obtained using a slide caliper 10, 17 and 21 days after inoculation and then tumor volumes were calculated using the formula 0.5 x (A x B^2), where A and B are the longest and shortest dimensions of the tumor, respectively (Andre et al. 2002). Six-hundred microliters of plasma were collected from tumor-bearing mice sacrificed at 10, 17 and 21 days after inoculation.

4.7. Immunohistochemistry staining

Frozen HARA-B tumor tissues in 5 µm thick sections were fixed in 4% paraformaldehyde for 15 min at 4 °C. Heat-induced epitope retrieval was performed in the Target Retrieval Solution pH 9 (Dako) according to the manufacturer's instructions. After the epitope retrieval, endogenous peroxidase was blocked with the Peroxidase Blocking Reagent (Dako). Following peroxidase blocking, the slides were incubated with 10% BSA solution for 30 min at room temperature. After BSA blocking, the slides were incubated for 60 min with goat anti human EGFR polyclonal antibody, 5 µg/ml in 3% BSA at room temperature. After 3 washes with Wash Buffer (Dako), each slide was incubated for 60 min with HRP-conjugated anti-goat IgG antibody diluted 1:1,000 in 3% BSA at room temperature. After the final 3 washes with wash buffer, the slides were stained with 3,3'-diaminobenzidine. After development, the slides were lightly counterstained with Mayer's hematoxylin. All procedures were performed using AutoStainer (Dako).

4.8. Statistical analysis

Statistical significance in ELISA signals between the control and target groups was analyzed using the one-way ANOVA followed by Tukey post-hoc test.

Acknowledgements: This study was supported in part by Grants-in-Aid for Scientific Research from the Ministry of Education, Culture, Sports, Science and Technology of Japan, and from the Japan Society for the Promotion of

Science (JSPS). This study was also supported in part by Health Labor Sciences Research Grants from the Ministry of Health, Labor and Welfare of Japan.

References

Abache T, Le Naour F, Planchon S, Harper F, Boucheix C, Rubinstein E (2007) The transferrin receptor and the tetraspanin web molecules CD9, CD81, and CD9P-1 are differentially sorted into exosomes after TPA treatment of K562 cells. J Cell Biochem 102: 650–664.

Andre F, Schartz NE, Movassagh M, Flament C, Pautier P, Morice P, Pomel C, Lhomme C, Escudier B, Le Chevalier T, Tursz T, Amigorena S, Raposo G, Angevin E, Zitvogel L (2002) Malignant effusions and immunogenic tumour-derived exosomes. Lancet 360: 295–305.

Carloni V, Mazzocca A, Ravichandran KS (2004) Tetraspanin CD81 is linked to ERK/MAPKinase signaling by Shc in liver tumor cells. Oncogene 23: 1566–1574.

Chairoungdua A, Smith DL, Pochard P, Hull M, Caplan MJ (2010) Exosome release of beta-catenin: a novel mechanism that antagonizes Wnt signaling. J Cell Biol 190: 1079–1091.

Chiba M, Kimura M, Asari S (2012) exosomes secreted from human colorectal cancer cell lines contain mRNAs, microRNAs and natural antisense RNAs, that can transfer into the human hepatoma HepG2 and lung cancer A549 cell lines. Oncol Rep 28: 1551–1558.

Deng Z, Cheng Z, Xiang X, Yan J, Zhuang X, Liu C, Jiang H, Ju S, Zhang L, Grizzle W, Mobley J, Roman J, Miller D, Zhang HG (2012) Tumor cell cross talk with tumor-associated leukocytes leads to induction of tumor exosomal fibronectin and promotes tumor progression. Am J Pathol 180: 390–398.

Fevrier B, Vilette D, Archer F, Loew D, Faigle W, Vidal M, Laude H, Raposo G (2004) Cells release prions in association with exosomes. Proc Natl Acad Sci U S A 101: 9683–9688.

Gusterson B, Cowley G, Smith JA, Ozanne B (1984) Cellular localisation of human epidermal growth factor receptor. Cell Biol Int Rep 8: 649–658.

Jacot W, Pujol JL, Boher JM, Lamy PJ (2004) Serum EGF-receptor and HER-2 extracellular domains and prognosis of non-small-cell lung cancer. Br J Cancer 91: 430–433.

Kosaka N, Iguchi H, Yoshioka Y, Takeshita F, Matsuki Y, Ochiya T (2010) Secretory mechanisms and intercellular transfer of microRNAs in living cells. J Biol Chem 285: 17442–17452.

Logozzi M, De Milito A, Lugini L, Borghi M, Calabrò L, Spada M, Perdicchio M, Marino ML, Federici C, Iessi E, Brambilla D, Venturi G, Lozupone F, Santinami M, Huber V, Maio M, Rivoltini L, Fais S (2009) High levels of exosomes expressing CD63 and caveolin-1 in plasma of melanoma patients. PLoS One 4: e5219.

MacSween JM, Warner NL, Bankhurst AD, Mackay IR (1972) Carcinoembryonic antigen in whole serum. Br J Cancer 26: 356–360.

Mathivanan S, Lim JW, Tauro BJ, Ji H, Moritz RL, Simpson RJ (2010) Proteomics analysis of A33 immunoaffinity-purified exosomes released from the human colon tumor cell line LIM1215 reveals a tissue-specific protein signature. Mol Cell Proteomics 9: 197–208.

Modjtahedi H, Eccles SA, Box G, Styles J, Dean CJ (1993) Antitumor activity of combinations of antibodies directed against different epitopes on the extracellular domain of the human EGF receptor. Cell Biophys 22: 129–146.

Philip R, Carrington L, Chan M (2011) US FDA perspective on challenges in co-developing *in vitro* companion diagnostics and targeted cancer therapeutics. Bioanalysis 3: 383–389.

Pols MS, Klumperman (2009) Trafficking and function of the tetraspanin CD63. Exp Cell Res 315: 1584–1592.

Pujol JL, Grenier J, Daurès JP, Daver A, Pujol H, Michel FB (1993) Serum fragment of cytokeratin subunit 19 measured by CYFRA 21–1 immunoradiometric assay as a marker of lung cancer. Cancer Res 53: 61–66.

Simons M, Raposo G (2009) Exosomes–vesicular carriers for intercellular communication. Curr Opin Cell Biol 21: 575–581.

Simpson RJ, Jensen SS, Lim JW (2008) Proteomic profiling of exosomes: current perspectives. Proteomics 8: 4083–4099.

Skog J, Würdinger T, van Rijn S, Meijer DH, Gainche L, Sena-Esteves M, Curry WT Jr, Carter BS, Krichevsky AM, Breakefield XO (2008) Glioblastoma microvesicles transport RNA and proteins that promote tumour growth and provide diagnostic biomarkers. Nat Cell Biol 10: 1470–1476.

Taylos DD, Gercel-Taylos C (2008) MicroRNA signatures of tumor-derived exosomes as diagnostic biomarkers of ovarian cancer. Gynecol Oncol 110: 13–21.

Théry C, Ostrowski M, Segura E (2009) Membrane vesicles as conveyors of immune responses. Nat Rev Immunol 9: 581–593.

Valadi H, Ekström K, Bossios A, Sjöstrand M, Lee JJ, Lötvall JO (2007) Exosome-mediated transfer of mRNAs and microRNAs is a novel mechanism of genetic exchange between cells. Nat Cell Biol 9: 654–659.

Witek RP, Yang L, Liu R, Jung Y, Omenetti A, Syn WK, Choi SS, Cheong Y, Fearing CM, Agboola KM, Chen W, Diehl AM (2009) Liver cell-derived microparticles activate hedgehog signaling and alter gene expression in hepatic endothelial cells. Gastroenterology 136: 320–330 e2.

Liver-specific microRNAs as biomarkers of nanomaterial-induced liver damage

IOP PUBLISHING NANOTECHNOLOGY
Nanotechnology **24** (2013) 405102 (7pp) doi:10.1088/0957-4484/24/40/405102

Liver-specific microRNAs as biomarkers of nanomaterial-induced liver damage

Takashi Nagano[1,6], Kazuma Higashisaka[1,6], Akiyoshi Kunieda[1], Yuki Iwahara[1], Kota Tanaka[1], Kazuya Nagano[2], Yasuhiro Abe[3], Haruhiko Kamada[2,4], Shin-ichi Tsunoda[2,4], Hiromi Nabeshi[5], Tomoaki Yoshikawa[1], Yasuo Yoshioka[1,7] and Yasuo Tsutsumi[1,2,4,7]

[1] Laboratory of Toxicology and Safety Science, Graduate School of Pharmaceutical Sciences, Osaka University, 1-6 Yamadaoka, Suita, Osaka 565-0871, Japan
[2] Laboratory of Biopharmaceutical Research, National Institute of Biomedical Innovation, 7-6-8, Saito-Asagi, Ibaraki, Osaka 567-0085, Japan
[3] Cancer Biology Research Center, Sanford Research/USD, Sioux Falls, SD, USA
[4] The Center for Advanced Medical Engineering and Informatics, Osaka University, 1-6, Yamadaoka, Suita, Osaka 565-0871, Japan
[5] Division of Foods, National Institute of Health Sciences, Tokyo, Japan

E-mail: yasuo@phs.osaka-u.ac.jp and ytsutsumi@phs.osaka-u.ac.jp

Received 9 May 2013, in final form 23 August 2013
Published 12 September 2013
Online at stacks.iop.org/Nano/24/405102

Abstract
Although nanomaterials are being used in various fields, their safety is not yet sufficiently understood. We have been attempting to establish a nanomaterials safety-assessment system by using biomarkers to predict nanomaterial-induced adverse biological effects. Here, we focused on microRNAs (miRNAs) because of their tissue-specific expression and high degree of stability in the blood. We previously showed that high intravenous doses of silica nanoparticles of 70 nm diameter (nSP70) induced liver damage in mice. In this study, we compared the effectiveness of serum levels of liver-specific or -enriched miRNAs (miR-122, miR-192, and miR-194) with that of conventional hepatic biomarkers (alanine aminotransferase (ALT) and aspartate aminotransferase (AST)) as biomarkers for nSP70. After mice had been treated with nSP70, their serum miRNAs levels were measured by using quantitative RT-PCR. Serum levels of miR-122 in nSP70-treated mice were the highest among the three miRNAs. The sensitivity of miR-122 for liver damage was at least as good as those of ALT and AST. Like ALT and AST, miR-122 may be a useful biomarker of nSP70. We believe that these findings will help in the establishment of a nanomaterials safety-assessment system.

1. Introduction

Nanomaterials are defined as substances that have at least one dimension less than 100 nm long. They are now widely used in cosmetics, foods, and medicines because they possess innovative functions such as high electrical conductivity, tensile strength, and tissue permeability [1, 2]. However, with the development of nanomaterials has come concern that, unlike the case with microsized materials, their unique characteristics may induce unexpected biological responses [3–5]. For example, recent reports have shown that carbon nanotubes can induce mesothelioma-like lesions in mice, similar to those induced by asbestos [6]. In addition, our group has shown that silica nanoparticles with a diameter of 70 nm (nSP70) can induce severe liver damage and pregnancy complications in mice, and reactive oxygen species (ROS) generation and DNA damage *in vitro*, whereas microsized silica particles do not have these effects [7–10]. Nevertheless, because nanomaterials have the potential to improve our quality of life, it is important that we develop and promote the use of safe forms. Furthermore, the development of

[6] These authors contributed equally to the work.
[7] Address for correspondence: Laboratory of Toxicology and Safety Science, Graduate School of Pharmaceutical Sciences, Osaka University, 1-6 Yamadaoka, Suita, Osaka 565-0871, Japan.

biomarkers of the biological effects of nanomaterials would be invaluable for establishing a nanomaterials safety-assessment system and strategies for the development, production, and use of safe forms of nanomaterials. We have already explored biomarkers, with a focus on proteins, and have shown that acute-phase proteins such as haptoglobin, serum amyloid A, and C-reactive protein could be useful biomarkers of the biological effects of silica or platinum nanoparticles [11–13]. However, the use of proteins alone is not sufficient for predicting the adverse biological effects of nanomaterials, as we need to evaluate biomarkers consisting of other biological molecules.

microRNAs (miRNAs) are highly conserved and small (18- to 25-nucleotide) RNAs that play pivotal roles in gene expression—specifically at the post-transcriptional level—in plants and animals. In humans, miRNAs are involved in the regulation of development, cell differentiation, proliferation, and apoptosis [14, 15], because they regulate as many as one-third of all messenger RNAs (mRNAs) [16, 17]. Furthermore, recent reports have demonstrated that miRNAs would serve as useful biomarkers for the non-invasive, tissue-specific evaluation of diseases and drug-induced tissue damage [18, 19]. This is because they show tissue-specific expression [20, 21] and exist in a stable form in the blood, saliva, and urine [22–24].

From this perspective, we focused on miRNAs as biomarkers for predicting the biological effects of nanomaterials. Although there have been some analyses of the changes in miRNA expression following exposure to nanomaterials [25, 26], there have been very few attempts to use miRNAs as biomarkers of nanomaterials. We therefore need to collect systematic information on miRNAs as biomarkers so as to predict nanomaterials-induced biological effects and thus establish a nanomaterials safety-assessment system.

In this study, as a first trial, we attempted to investigate whether liver-specific or -enriched miRNAs (miR-122, miR-192, and miR-194) could be used as reliable biomarkers for liver damage induced by nSP70.

2. Materials and methods

2.1. Materials

Silica particles were purchased from micromod Partikeltechnologie (Rostock/Warnemünde, Germany). Silica particles with diameters of 70, 300, and 1000 nm (nSP70, nSP300, and mSP1000, respectively) were used. In addition, we used nSP70 modified with surface functional groups-a carboxyl group (nSP70-C) or an amino group (nSP70-N). The particles were sonicated for 5 min and then vortexed for 1 min before use. Lipopolysaccharide (LPS) and D-galactosamine hydrochloride (D-GalN) were purchased from Sigma-Aldrich (Tokyo, Japan).

2.2. Animals

Female BALB/c mice were purchased from Nippon SLC, Inc. (Shizuoka, Japan) and used at 6–7 weeks of age. All of the animal experimental procedures were performed in accordance with the Osaka University and National Institute of Biomedical Innovation guidelines for the welfare of animals.

2.3. Blood sample collection

BALB/c mice ($n = 5$ or 6 per group) were treated in various experiments with nSP70 at 10, 20, or 40 mg kg^{-1} or with nSP70-C, nSP70-N, nSP300, or mSP1000 at 40 mg kg^{-1}, via injection into the tail vein. As positive control of induction of liver damage, BALB/c mice ($n = 5$ or 6 per group) were intraperitoneally treated with LPS at 10 μg kg^{-1} and D-GalN at 700 mg kg^{-1}. Blood samples were collected at varying times (4, 8, 24, or 72 h after treatment) in several experiments. Sera were harvested by blood centrifugation at 8000*g* for 15 min.

2.4. Biochemical analysis

Serum levels of alanine aminotransferase (ALT) and aspartate aminotransferase (AST) were measured with a DRI-CHEM 7000 biochemical analyzer (Fujifilm Corp., Tokyo, Japan).

2.5. Isolation of total RNA from serum

We extracted total RNA, including small RNA, from serum samples by using a miRNeasy Mini Kit (QIAGEN, Tokyo, Japan) in accordance with the manufacturer's instructions. In brief, 250 μl of QIAzol lysis reagent was added to 50 μl of serum. After the addition of 50 μl of chloroform, the samples were mixed completely and centrifuged. Then, 100 μl of supernatant was transferred to a new tube and mixed with 150 μl of 100% ethanol. The sample was then applied directly to a RNeasy Mini spin column (QIAGEN) and the combined RNA to column was cleaned with wash buffers to remove impurities. Total RNA was eluted in 30 μl of RNase-free water.

2.6. Real-time quantitative reverse-transcription PCR (qRT-PCR)

Serum levels of miR-122, miR-192, and miR-194 were measured by using TaqMan RT-PCR. Each miRNA in 5 μl of purified total RNA was reverse transcribed with a miRNA-specific stem-loop reverse transcriptase primer (Life Technologies, Tokyo, Japan). TaqMan RT-PCR was performed on a StepOne Plus real-time PCR system (Life Technologies, Tokyo, Japan). Generally, typical internal controls for miRNA expression, such as U6 RNA and 5S rRNA, are degraded in serum samples [27]. Therefore, we equalized all of the conditions and then normalized the levels of each miRNA by serum volume. The expression level of each miRNA is shown as a relative fold-change. Relative expression was compared between the silica-particle-treated group and the untreated group.

2.7. Statistical analyses

All results are expressed as means $\pm$ SEM differences were compared by using the Student's *t*-test or Bonferroni test after ANOVA (analysis of variance).

3. Results

3.1. Physicochemical properties of silica nanoparticles

Silica nanoparticles are common nanomaterials that are being used in cosmetics, foods, and medicines [28, 29]. Considering that further use of silica nanoparticles is expected, it is important to assess their safety. We used silica particles with diameters of 70 nm (nSP70), 300 nm (nSP300), and 1000 nm (mSP1000), as well as nSP70 with carboxyl (nSP70-C) or amino (nSP70-N) surface functional groups. In our previous study, we confirmed by transmission electron microscopy that all silica particles of the above-listed sizes and types were smooth-surfaced spheres [7–10]. We have already shown that the hydrodynamic diameters of nSP70, nSP70-C, nSP70-N, nSP300, and mSP1000 are 64.6, 69.6, 71.8, 322, and 1140 nm, respectively, and their zeta potentials (overall surface potentials) are −52.7, −76.3, −29.0, −62.1, and −67.0 mV, respectively [7–10]. The carboxyl and amino surface modifications therefore altered the surface charge of the nSP70 particles. In addition, we have already shown that the size-distribution spectrum of each set of silica particles had a single peak, and the measured hydrodynamic diameter corresponded almost precisely to the primary particle size of each set of silica particles [7–10]. These results indicated that the silica particles used in this study were well dispersed in solution.

3.2. Liver-specific or -enriched miRNAs as biomarkers of silica nanoparticles

To evaluate the usefulness of microRNAs (miRNAs) as biomarkers for nanomaterials, we focused on a model of liver damage induced by nSP70. We have previously shown that treatment of mice with high-dose nSP70 intravenously via the tail vein induced lethal toxicity and severe liver damage. Therefore, we assessed the usefulness of the liver-specific or -enriched miRNAs miR-122, miR-192, and miR-194 as biomarkers of liver damage. miR-122 and miR-192 are the two miRNAs expressed most abundantly in the human liver [30], and hepatic miR-194 is highly expressed in hepatic epithelial cells, including hepatocytes, which are parenchymal cells and account for more than 80% of liver cells [31]. Therefore, to collect systematic information on whether miRNAs have the potential to be biomarkers of nanomaterials, we selected those three major miRNAs in liver. Mice were given nSP70, nSP300, or mSP1000 via the tail vein. A dose rate of 40 mg kg^{-1} was chosen, because in the case of nSP70 this dose rate significantly increases the levels of ALT and AST [10]. As positive control, mice were intraperitoneally treated with LPS and D-GalN. At 8 h after treatment, we evaluated the serum level of each miRNA by using qRT-PCR and those of ALT and AST (i.e. the conventional hepatic biomarkers) by using biochemical analysis. The levels of miR-122 (figure 1(A)), ALT (figure 1(B)), and AST (figure 1(C)) in LPS/D-GalN-treated mice were significantly increased compared to those of vesicle-treated mice. The levels of miR-122 (figure 1(A)) and miR-192 (figure 1(D)) in nSP70-treated mice were significantly greater than those in saline-, nSP300- or mSP1000-treated mice and untreated mice. In contrast, the serum levels of miR-194 did not differ significantly among any groups (figure 1(E)). In addition, the levels of ALT (figure 1(B)) and AST (figure 1(C)) in nSP70-treated mice were significantly greater than those in saline-, nSP300- or mSP1000-treated mice and untreated mice. Thus, miR-122 and miR-192 may be useful as biomarkers for evaluating liver damage induced by nSP70. We focused on miR-122 in the following assessment, because it had the highest rate of expression among the three miRNAs.

3.3. Sensitivity and time-dependency of miR-122 expression

To more precisely assess the serum levels of miR-122 as a biomarker, we examined the sensitivity and time-dependency of miR-122 expression after treatment with nSP70. Mice were intravenously treated with nSP70 at 10, 20, or 40 mg kg^{-1}. Blood samples were collected 8 h after treatment and the levels of miR-122, ALT, and AST were measured. The serum levels of miR-122 (figure 2(A)), ALT (figure 2(B)), and AST (figure 2(C)) showed dose-dependent patterns of expression. In mice treated with 40 mg kg^{-1} nSP70 and 20 mg kg^{-1} in the case of AST, the levels of all three markers were significantly greater than in untreated or saline-treated mice. Thus, as was the case with ALT and AST, the increase in serum miR-122 levels was dependent on the dose of nSP70. Next, to assess the time-dependency of miR-122 expression, we examined the serum levels of miR-122 (figure 2(D)), ALT (figure 2(E)), and AST (figure 2(F)) at 4, 8, 24, and 72 h after intravenous injection of nSP70 at 40 mg kg^{-1}. The serum levels of miR-122 in nSP70-treated mice were significantly higher than those in saline-treated mice at every time point, as was the case with ALT and AST. These results suggested that the pattern of release of miR-122 into the blood was the same as those of ALT and AST.

3.4. miR-122 response after treatment of mice with surface-modified nSP70

Our group has previously demonstrated that modification of nSP70 with surface functional groups such as a carboxyl group (nSP70-C) or amino group (nSP70-N) can reduce the toxic effects of nSP70 (e.g., pregnancy complications in mice and ROS generation and DNA damage *in vitro*) [8, 9]. Here, we tested the use of miR-122 as a biomarker to determine whether the safety of nSP70 could be improved by adding functional groups. BALB/c mice were treated intravenously with nSP70, nSP70-C, or nSP70-N at 40 mg kg^{-1}. At 8 h after treatment, we measured the levels of miR-122 (figure 3(A)), ALT (figure 3(B)), and AST (figure 3(C)). The serum levels of miR-122 in nSP70-C- or nSP70-N-treated mice were significantly lower than that in nSP70-treated mice and were almost the same as those in untreated or saline-treated mice. The serum levels of ALT after treatment with nSP70-C or nSP70-N showed a trend similar to those of miR-122. In contrast, although the level of AST in nSP70-N-treated mice was significantly lower than that in nSP70-treated mice, the

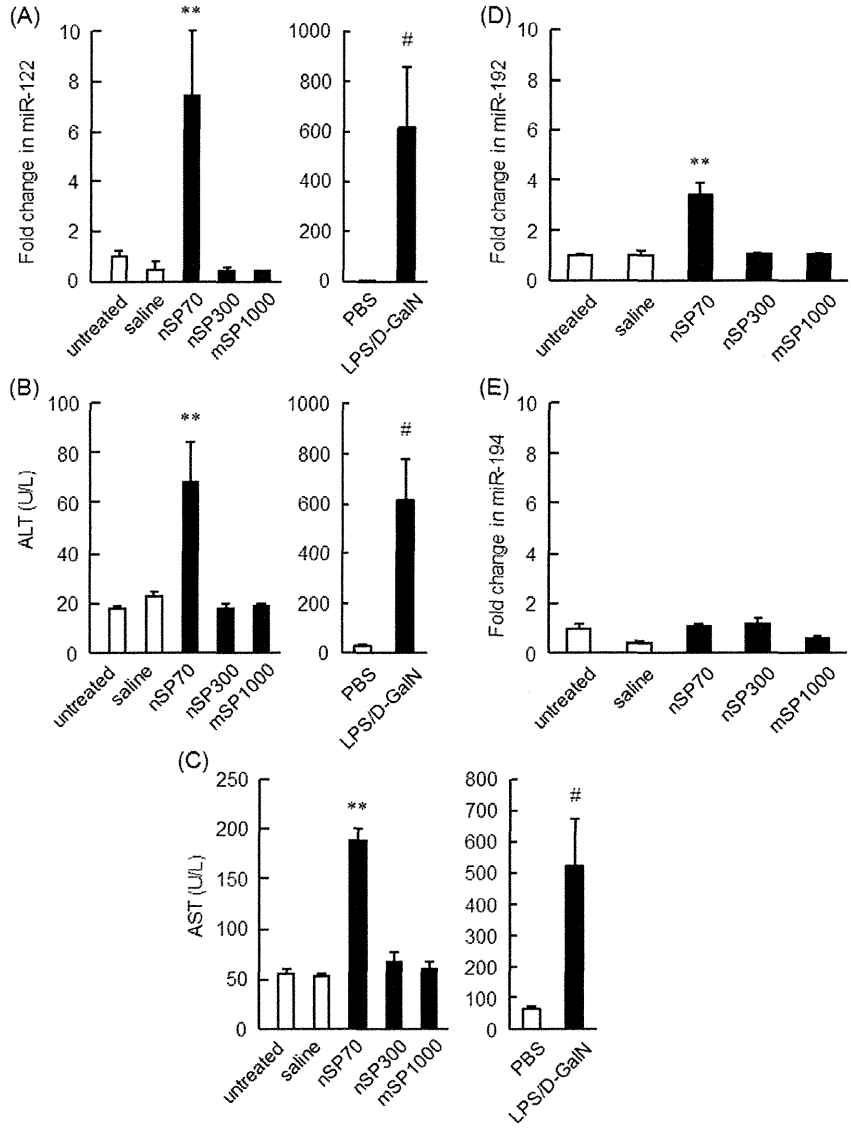

Figure 1. Usefulness of liver-specific microRNAs (miR-122, miR-192, and miR-194) as biomarkers for the development of safe silica nanoparticles. BALB/c mice were intravenously treated with nSP70, nSP300, or mSP1000 at 40 mg kg^{-1}. In addition, as positive control, mice were intraperitoneally treated with LPS and D-GalN. After 8 h, the serum levels of each microRNA, (A) miR-122, (D) miR-192, and (E) miR-194, were examined by real-time quantitative reverse-transcription PCR. Serum levels of (B) alanine aminotransferase (ALT) and (C) aspartate aminotransferase (AST) were measured by biochemical analysis. Data are presented as means ± SEM ($n = 6$; $^{**}P < 0.01$ versus value for saline-, nSP300-, mSP1000-treated group and untreated group by ANOVA; $^{\#}P < 0.05$ versus value for PBS-treated group by Student's *t*-test).

AST level in nSP70-C-treated mice was significantly greater than that in untreated or saline-treated mice. These results suggest that serum miR-122 may be useful as a biomarker for assessing improvement of the safety of nSP70 through surface modification.

4. Discussion

Our group showed previously that nSP70 can induce severe liver damage in mice [10]. Here, we examined whether liver-specific or -enriched miRNAs (miR-122, miR-192, and miR-194) were potentially useful as biomarkers of the liver damage induced by nSP70. Although miR-192 and miR-194 are thought to be involved in controlling proliferation and metastasis in liver cancer, the details of their functions are less well understood than in the case of miR-122 [31]. miR-122 is a key regulator of cholesterol and fatty-acid metabolism in the liver [32]. Therefore, it is likely that changes in the levels of miR-122 will predict not only liver damage but also the biological effects of that damage, such as abnormalities in fat metabolism. In addition, miR-122 has also been shown to be biomarkers for drug-induced liver injury in mice, rats, and human [33–35].

First, we showed that serum levels of miR-122 and miR-192 in nSP70-treated mice were elevated 8 h after treatment (figures 1(A) and (D)), as were those of ALT and AST (figures 1(B) and (C)), and that the levels of miR-122

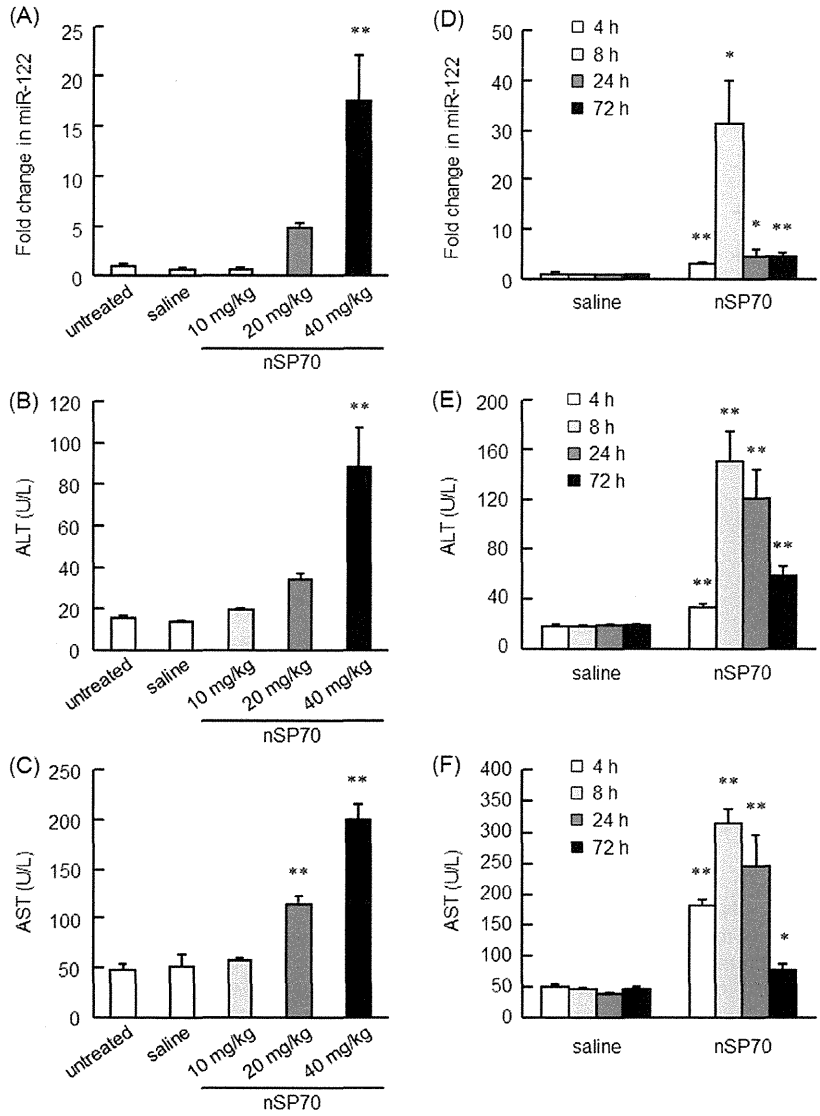

Figure 2. Serum levels of miR-122 after treatment with nSP70. BALB/c mice were intravenously treated with nSP70 at 10, 20, or 40 mg kg^{-1}. At 8 h after treatment with nSP70, the levels of (A) miR-122, (B) alanine aminotransferase (ALT), and (C) aspartate aminotransferase (AST) were analyzed. In addition, at 4, 8, 24, and 72 h after treatment with nSP70 at 40 mg kg^{-1}, the levels of (D) miR-122, (E) ALT, and (F) AST were examined. Data are presented as means ± SEM ($n = 5$ or 6; $^{*}P < 0.05$, $^{**}P < 0.01$ versus value for saline-treated group and untreated group by ANOVA).

were much higher than those of miR-192. We considered that this was because miR-122 accounts for 70% of all liver miRNA. By contrast, the serum levels of miR-194 in nSP70-treated mice did not differ significantly from those in untreated or saline-treated mice (figure 1(E)). The expression of miR-194 may change markedly with time; because we analyzed this expression only at 8 h after treatment, further time-course studies are needed before this miRNA can be discarded as a biomarker.

The serum levels of ALT and AST in mice treated with nSP70 at 40 mg kg^{-1} were beyond the physiological range, at about 4 times the values in untreated or saline-treated mice. In contrast, the serum level of miR-122 in nSP70-treated mice was about 15 times that in untreated or saline-treated mice (figures 2(A)–(C)). This suggests that miR-122 may be a more sensitive biomarker than the currently used ALT and AST in detecting liver damage induced by nSP70. In addition, as shown in figures 2(A)–(C), we evaluated the dose-dependent expression of miR-122 only at 8 h after treatment with nSP70, and we showed that the pattern of expression of miR-122 was almost the same as that of ALT and AST. In another study, injection of acetaminophen did not cause serum ALT elevation at 1 h, although obvious increases in miR-122 and miR-192 levels were already observable [36]. Therefore, evaluation at time points earlier than 8 h after nSP70 injection with lower doses could reveal the possibility that miR-122 is a more sensitive predictor of nSP70-induced liver damage than ALT and AST.

As shown in figures 2(D)–(F), the serum levels of ALT and AST in mice treated with nSP70 at 24 h showed significantly greater than those in saline-treated mice, while for miRNA-122, it dropped at 24 h to the same level as

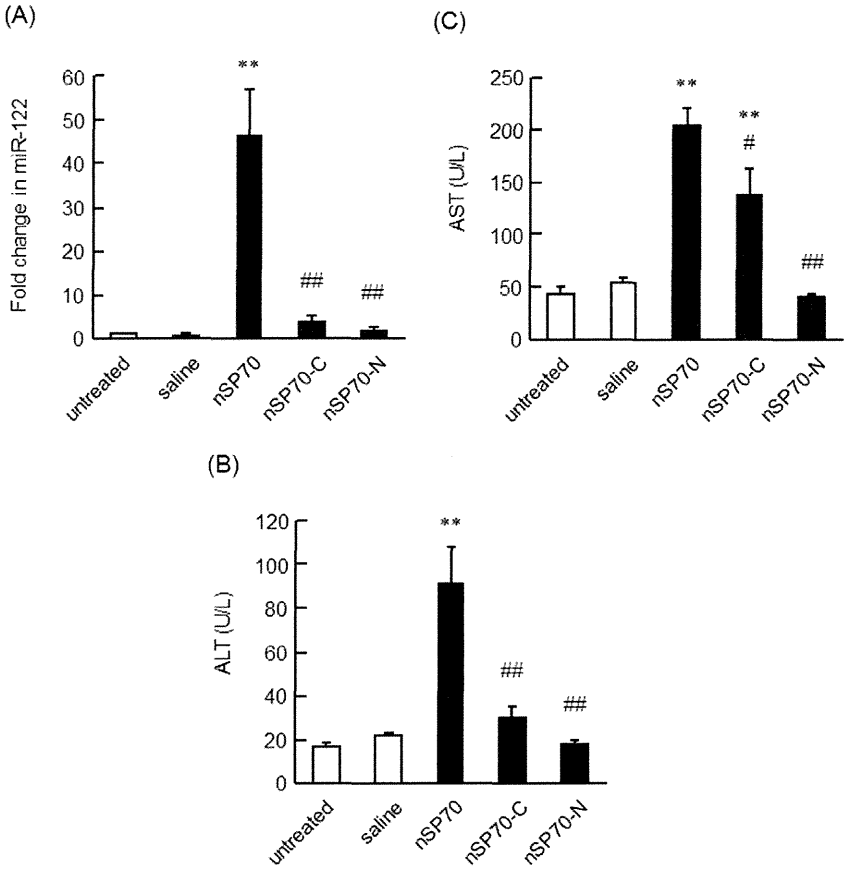

Figure 3. Responses of serum levels of miR-122 to treatment with surface-modified nSP70. BALB/c mice were intravenously treated with nSP70, nSP70-C, or nSP70-N at 40 mg kg^{-1}. Serum levels of (A) miR-122, (B) alanine aminotransferase (ALT), and (C) aspartate aminotransferase (AST) were measured 8 h after treatment. Data are presented as means ± SEM ($n = 5$ or 6; $^{**}P < 0.01$ versus value for saline-treated group and untreated group; $^{\#}P < 0.05$, $^{\#\#}P < 0.01$ versus value for nSP70-treated group by ANOVA).

72 h. In general, miRNAs are considered to be stable in the blood [37]. However, Yamaura *et al* showed that although miR-122 was stable in human plasma, it was unstable in rat plasma [38]. Therefore, although detailed information on the stability of mouse miR-122 is unavailable, it is possible that RNase action in the blood leads to a rapid decrease in miR-122 levels. Currently, there are two hypothetical pathways by which miRNAs can enter the circulation [39]. One is by direct leakage from cells, and the other is by release from cells via microvesicles. It is thought that direct secretion of miRNAs occurs in tissue damage or cell apoptosis [39]. We previously demonstrated that nSP70 administered via the tail vein was distributed mainly to the liver and induced cytotoxicity in primary hepatocytes isolated from nSP70-treated mice [7]. Taking these results together, it is conceivable that most miR-122 is leaked into the blood and degraded by RNase between 8 and 24 h after nSP70 treatment. On the other hand, the level of miR-122 in nSP70-treated mice showed significant increments compared to that of saline-treated mice over the time course of the experiment. Therefore, its change in expression over the full time course of the experiment was still useful for evaluating nSP70-induced liver damage. For these reasons, we consider that miR-122 is as useful as ALT and AST in evaluating nSP70-induced liver damage. However, because we cannot explain this in detail, we are now trying to investigate the mechanism involved.

Here, we evaluated the time course of miR-122 expression over only a short period of time after nSP70 treatment. However, considering that we are exposed to nanomaterials on a daily basis, there is a need to investigate the biological effects of long-term exposure to them. Recent reports have shown that long-term exposure to titanium dioxide nanomaterials in mice induces ROS production in the lung [40]. A nanomaterials safety-assessment system is required for the evaluation of not only acute effects but also chronic effects. Therefore, we intend to analyze nanomaterial-induced chronic biological effects by evaluating the long-term course of miRNA expression.

Although the levels of miR-122, ALT, and AST were lower in mice treated with modified nSP70 than in those treated with unmodified nSP70 (figure 3), the AST level in nSP70-C-treated mice was higher than that in untreated mice. It is possible that nSP70-C and nSP70-N is safer than nSP70, because we previously demonstrated that differences in the surface charge state or kind of functional group of nanomaterials lead to different biological effects and cell responses [41–43]. On the other hand, AST is abundant not only in the liver but also in the skeletal muscle, heart, and kidney. Taking these results together, we consider that the

increase in AST in nSP70-C-treated mice was attributable to damage to tissues other than the liver. We are now analyzing in detail the effects of nanomaterials by focusing on other tissues.

This study is just the first step in the development of a miRNA-based safety-assessment system for nanomaterials. We have shown here that miR-122 is almost as useful as ALT and AST as a biomarker for nanomaterials. Recent reports have shown that many miRNAs exist not only in blood but also in other body fluids such as urine or saliva [22, 23]. In light of these reports, we consider that miR-122 might have the potential to predict nSP70-induced liver damage non-invasively from analyses of urine or saliva. In addition, many tissue-specific miRNAs other than miR-122 have been reported [44]. Therefore, to develop more specific or more sensitive biomarkers than the established system, there is a strong need for comprehensive analyses of the miRNAs associated with various tissues, such as brain and pancreas, for which we do not have enough useful biomarkers. Considering that miRNAs regulate the expression of the mRNAs involved in protein translation, identifying the changes that occur in miRNA expression upon exposure to nanomaterials will enable us to predict the biological effects of these materials. We are now trying comprehensively to explore those miRNAs that show changes in expression levels upon exposure to nanomaterials. We hope that these studies will help to establish a system for evaluating the safety and usefulness of nanomaterials.

5. Conclusions

We have revealed here that miR-122 and miR-192 may be useful biomarkers of liver damage induced by nSP70. miR-122, in particular, may be comparable to ALT and AST as a biomarker for this purpose.

Acknowledgments

This study was supported, in part, by Grants-in-Aid for Scientific Research from the Ministry of Education, Culture, Sports, Science and Technology of Japan (MEXT) and from the Japan Society for the Promotion of Science (JSPS); and by the Knowledge Cluster Initiative (MEXT); by Health Labour Sciences Research Grants from the Ministry of Health, Labour and Welfare of Japan (MHLW); by a Global Environment Research Fund from the Ministry of the Environment; by Food Safety Commission, Japan; by the Cosmetology Research Foundation; by the Smoking Research Foundation; by the Research Foundation for Pharmaceutical Sciences; by the Japan Food Chemical Research Foundation; and by the Takeda Science Foundation.

References

[1] Kaur I P and Agrawal R 2007 *Recent Pat. Drug Deliv. Formul.* **1** 171–82
[2] Cormode D P, Jarzyna P A, Mulder W J and Fayad Z A 2010 *Adv. Drug Deliv. Rev.* **62** 329–38
[3] Nel A, Xia T, Madler L and Li N 2006 *Science* **311** 622–7
[4] Donaldson K, Murphy F A, Duffin R and Poland C A 2010 *Part. Fibre Toxicol.* **7** 5
[5] Shvedova A A, Kagan V E and Fadeel B 2010 *Annu. Rev. Pharmacol. Toxicol.* **50** 63–88
[6] Poland C A *et al* 2008 *Nature Nanotechnol.* **3** 423–8
[7] Nabeshi H *et al* 2011 *Biomaterials* **32** 2713–24
[8] Yamashita K *et al* 2011 *Nature Nanotechnol.* **6** 321–8
[9] Nabeshi H *et al* 2011 *Part. Fibre Toxicol.* **8** 1
[10] Nabeshi H *et al* 2012 *Nanotechnology* **23** 045101
[11] Higashisaka K *et al* 2011 *Biomaterials* **32** 3–9
[12] Higashisaka K *et al* 2012 *Nanoscale Res. Lett.* **7** 555
[13] Nagano T *et al* 2012 *Pharmazie* **67** 958–9
[14] Schickel R, Boyerinas B, Park S M and Peter M E 2008 *Oncogene* **27** 5959–74
[15] Cordes K R and Srivastava D 2009 *Circ. Res.* **104** 724–32
[16] Esquela-Kerscher A and Slack F J 2006 *Nature Rev. Cancer* **6** 259–69
[17] Pauley K M, Cha S and Chan E K 2009 *J. Autoimmun.* **32** 189–94
[18] Kosaka N, Iguchi H and Ochiya T 2010 *Cancer Sci.* **101** 2087–92
[19] Brase J C, Wuttig D, Kuner R and Sultmann H 2010 *Mol. Cancer* **9** 306
[20] Lagos-Quintana M, Rauhut R, Yalcin A, Meyer J, Lendeckel W and Tuschl T 2002 *Curr. Biol.* **12** 735–9
[21] Aboobaker A A, Tomancak P, Patel N, Rubin G M and Lai E C 2005 *Proc. Natl Acad. Sci. USA* **102** 18017–22
[22] Michael A, Bajracharya S D, Yuen P S, Zhou H, Star R A, Illei G G and Alevizos I 2010 *Oral Dis.* **16** 34–8
[23] Hanke M, Hoefig K, Merz H, Feller A C, Kausch I, Jocham D, Warnecke J M and Sczakiel G 2010 *Urol. Oncol.* **28** 655–61
[24] Yamada Y *et al* 2011 *Cancer Sci.* **102** 522–9
[25] Halappanavar S, Jackson P, Williams A, Jensen K A, Hougaard K S, Vogel U, Yauk C L and Wallin H 2011 *Environ. Mol. Mutagen.* **52** 425–39
[26] Burklew C E, Ashlock J, Winfrey W B and Zhang B 2012 *PLoS One* **7** e34783
[27] Cortez M A and Calin G A 2009 *Exp. Opin. Biol. Ther.* **9** 703–11
[28] Knopp D, Tang D and Niessner R 2009 *Anal. Chim. Acta* **647** 14–30
[29] Peters R *et al* 2012 *ACS Nano* **6** 2441–51
[30] Hou J *et al* 2011 *Cancer Cell* **19** 232–43
[31] Meng Z, Fu X, Chen X, Zeng S, Tian Y, Jove R, Xu R and Huang W 2010 *Hepatology* **52** 2148–57
[32] Rotllan N and Fernandez-Hernando C 2012 *Cholesterol* **2012** 847849
[33] Wang K, Zhang S, Marzolf B, Troisch P, Brightman A, Hu Z, Hood L E and Galas D J 2009 *Proc. Natl Acad. Sci. USA* **106** 4402–7
[34] Starkey Lewis P J *et al* 2011 *Hepatology* **54** 1767–76
[35] Starckx S *et al* 2013 *Toxicol. Pathol.* **41** 795–804
[36] Shi Q, Yang X and Mendrick D L 2013 *Biomark. Med.* **7** 307–15
[37] Gilad S *et al* 2008 *PLoS One* **3** e3148
[38] Yamaura Y, Nakajima M, Takagi S, Fukami T, Tsuneyama K and Yokoi T 2012 *PLoS One* **7** e30250
[39] Zen K and Zhang C Y 2012 *Med. Res. Rev.* **32** 326–48
[40] Sun Q *et al* 2012 *J. Biomed. Mater. Res.* A **100** 2554–62
[41] Nabeshi H *et al* 2011 *Nanoscale Res. Lett.* **6** 93
[42] Morishige T *et al* 2012 *Arch. Toxicol.* **86** 1297–307
[43] Yoshida T *et al* 2012 *Biochem. Biophys. Res. Commun.* **427** 748–52
[44] Laterza O F *et al* 2009 *Clin. Chem.* **55** 1977–83